

# Self-Assembled Small-Molecule Microarrays for Protease Screening and Profiling

Hugo D. Urbina,<sup>[b]</sup> François Debaene,<sup>[a]</sup> Bernard Jost,<sup>[c]</sup> Christine Bole-Feysot,<sup>[c]</sup> Daniel E. Mason,<sup>[b]</sup> Petr Kuzmic,<sup>[d]</sup> Jennifer L. Harris,<sup>[b, e]</sup> and Nicolas Winssinger<sup>\*[a]</sup>

*Small-molecule microarrays are attractive for chemical biology as they permit the analysis of hundreds to thousands of interactions in a highly miniaturized format. Methods to prepare small-molecule microarrays from combinatorial libraries by a self-assembly process based on the sequence-specific hybridization of peptide nucleic acid (PNA) encoded libraries to oligonucleotide arrays are presented. A systematic study of the dynamic range for multiple detection agents, including direct fluorescence of attached fluorescein and cyanine-3 dyes, antibody-mediated fluorescence amplification, and biotin-gold nanoparticle detection, demonstrated that individual PNA-encoded probes can be detected to concentrations of 10 pM on the oligonucleotide microar-*

*rays. Furthermore, a new method for parallel processing of biological samples by using gel-based separation of probes is presented. The methods presented in this report are exemplified through profiling two closely related cysteine proteases, cathepsin K and cathepsin F, across a 625-member PNA-encoded tetrapeptide acrylate library. A series of the specific cathepsin K and F inhibitors identified from the library were kinetically characterized and shown to correlate with the observed microarray profile, thus validating the described methods. Importantly, it was shown that this method could be used to obtain orthogonal inhibitors that displayed greater than tenfold selectivity for these closely related cathepsins.*

## Introduction

Microarray-based technologies have attracted attention in chemical biology due to the fact that the miniaturized format is well suited to probe the millions of interactions that make up a biological organism. Several reports have already highlighted the potential benefits of small-molecule microarrays for the discovery of novel inhibitors or ligands.<sup>[1–3]</sup> Small-molecule microarrays have also been used to identify the substrate specificity of a protease or a kinase or even to measure the activity of enzymes in complex mixtures such as crude cell lysates.<sup>[4–8]</sup> An important consideration in the preparation of such a microarray is the choice of conditions to immobilize the small-molecule probe without compromising its biological function. A number of functional-group-specific chemistries have been developed to chemoselectively tether small molecules to the microarrays. Alternatively, libraries can be encoded with peptide nucleic acid (PNA) tags, such that libraries that exist as mixtures in solution self-assemble into an organized microarray through hybridization to DNA arrays.<sup>[9]</sup> This allows libraries synthesized by split-and-mix methods to be decoded in a single step. An advantage of this method compared to direct spotting of small molecules onto arrays is that the libraries can be used in solution for bioassays prior to self-assembly into the microarray format. Self-organized PNA-encoded small molecules also allow for a selection step prior to hybridization, thus providing alternative detection methods to those available with conventional spotted microarrays. Various methods can be suitable for the selection of probes interacting with proteins in biological samples; here we report a gel-based

method of separation that can be parallelized to accommodate multiple biological samples at once. This method was used to discover selective protease inhibitors for proteases of similar structure and substrate specificity. Proteases represent an interesting application of this technology as they have been implicated in a number of infectious diseases and other human

[a] F. Debaene,<sup>+</sup> Prof. N. Winssinger  
Institut de Science et Ingénierie Supramoléculaires, Université Louis Pasteur  
8 allée Gaspard Monge, 67000 Strasbourg (France)  
Fax: (+33) 390-245-112  
E-mail: winssinger@isis.u-strasbg.fr

[b] Dr. H. D. Urbina,<sup>+</sup> Dr. D. E. Mason, Dr. J. L. Harris  
Protease Biochemistry  
Genomics Institute of the Novartis Research Foundation  
10675 John Jay Hopkins Drive, San Diego, CA 92121 (USA)

[c] B. Jost, C. Bole-Feysot  
Plate-forme Biopuces de Strasbourg  
Institut de Génétique et de Biologie Moléculaire et Cellulaire  
Université Louis Pasteur  
Illkirch, Strasbourg (France)

[d] Dr. P. Kuzmic  
BioKin, Ltd.  
1652 S. Grand Avenue, Pullman, WA 99163 (USA)

[e] Dr. J. L. Harris  
Department of Molecular Biology, The Scripps Research Institute  
10550 N. Torrey Pines Road, San Diego, CA 92121 (USA)

[<sup>+</sup>] These authors contributed equally to this work.

 Supporting information for this article is available on the WWW under <http://www.chembiochem.org> or from the author.

pathologies<sup>[10]</sup> and access to specific inhibitors provides the means to study their role in such pathologies.

## Results and Discussion

### Oligonucleotide spotting, PNA hybridization, and detection

To allow for the widespread use of this PNA-encoding methodology, we have explored and optimized four important components of this technology; first, the spotting of short oligonucleotides on unfunctionalized slides so as to provide facile access to the necessary microarrays, second, the optimization of the hybridization conditions for PNA–DNA hybridization, third, the design of a general codon system applicable beyond the present library, and fourth, the optimization of the detection method.

Microarrays containing short oligonucleotides (20- to 30-mers) can be efficiently prepared by using photolithography, such as those commercially available from Affymetrix. However, the equipment or investment to obtain custom sequences on an array is substantial. On the other hand, microarrays prepared by contact printing require simpler instrumentation that can be more easily employed in a normal laboratory setting. However, such printed arrays have been prepared predominantly with long oligonucleotide sequences (copy DNA), where the oligonucleotide is immobilized by electrostatic interactions between a positively charged surface and the negatively charged DNA backbone. To allow for the use of shorter customized oligonucleotide sequences, a number of chemically derivatized glass surfaces have also been reported and commercialized that allow for the covalent immobilization of DNA onto the microarray surface. While this approach has given good results, it requires modified oligonucleotides with a reactive functionality (amino or thio) for the chemoselective reaction with the surface. A potentially simpler approach would be to immobilize short unmodified oligonucleotides through photocrosslinking. A concern with this strategy was that the crosslinking of nucleotides involved in the PNA:DNA hybridization to the surface of a chip may interfere with hybridization. To evaluate the extent of this potential issue, a series of 14-mer PNA sequences were hybridized on microarrays prepared by UV crosslinking of 40-mer or 25-mer unmodified oligonucleotides. The intensity and dynamic range of hybridization was comparable in both cases, which suggests that the crosslinking does not interfere substantially with hybridization. To optimize the spotting conditions prior to photocrosslinking, a series of tests utilizing either saline sodium citrate (SSC; 150 mM NaCl, 15 mM Na citrate) or dimethylsulfoxide (DMSO) in varying concentrations were used to spot the oligonucleotides (see Figure S1 in the Supporting Information). The results show that, while both solvent systems can be used for oligonucleotide spotting, an important variable for good spot morphology is the humidity. At 75% humidity, DMSO spots became diffuse with poor morphology, while SSC-containing oligonucleotide spots were clearly superior to DMSO spots. On the other hand, when the oligonucleotides were spotted at 40–45% humidity, the DMSO-containing spots showed better morphology than

the SSC-containing spots. A likely explanation for this observation may be that, because DMSO has a slow evaporation rate, it requires a lower relative-humidity environment to maintain spot morphology after deposition on a slide than SSC. The poor spot morphology for DMSO seen at 75% relative humidity may be explained by the hygroscopic nature of DMSO, so that at such a high humidity level some water is taken up by the deposited spot, thus adversely affecting spot morphology. Therefore, the local relative humidity must be taken into account when selecting an oligonucleotide-spotting buffer system if a humidity-controlled chamber is not available.

The conditions were next optimized for the PNA:DNA hybridization in the microarray format. It is known that, unlike DNA/DNA interaction, DNA/PNA interaction is not very sensitive to salt concentration. Nevertheless, high salt concentration can be detrimental as it leads to solubility problems with the PNA. The buffers that were investigated minimized salt content and relied on formamide to modulate the hybridization conditions. For instance, formamide at a concentration of 40% was significantly better at reducing nonspecific binding than 28% formamide in an otherwise similar hybridization mixture (see Figure S2 in the Supporting Information).

We then turned our attention to the codon system used to encode the library. In our previous experience, we found it to be essential that the solution set of all permutations of the codons falls within a narrow distribution of the melting temperature ( $T_m$ ) to insure homogeneous detection of every library member at a given concentration. The codon system (Figure 1 A) was designed based on our previous codon system<sup>[7,8]</sup>

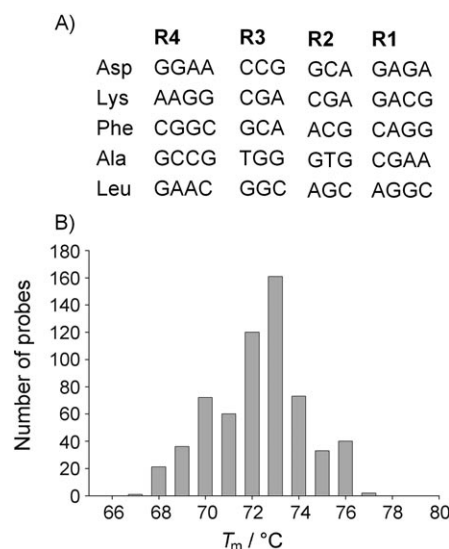


**Figure 1.** A) Sequence of the codon system for the PNA-encoded libraries. B) Histogram of predicted  $T_m$  values for all combinatorial PNA tags (y axis: number of probes, x axis:  $T_m$  value).

with the aim of minimizing  $T_m$  distribution of the solution set while also minimizing undesired cross-hybridization and problematic sequences such as hairpin sequences or sequences containing more than six contiguous purine residues. We had

previously observed that one base-pair mismatch was not sufficient to reliably avoid cross-hybridization and that the first and last codon are more susceptible to give rise to cross-hybridization. With these considerations in mind, we designed a codon system where all codons differ by at least two base-pair mismatches and the first and last codons have four nucleotides rather than three (Figure 1A). Analysis of the predicted<sup>[11]</sup>  $T_m$  values of the solution set of every combinatorial 14-mer showed that the lowest calculated  $T_m$  value was 68 °C and the highest calculated  $T_m$  value was 77 °C, with more than 75% of the library falling within a 5 °C distribution (Figure 1B). To test this codon system experimentally, four representative PNA sequences with calculated  $T_m$  values of 70, 72, 73, and 76 °C were synthesized and hybridized by using the optimized conditions. The dynamic range of hybridization was investigated by using four different detection methods: direct quantification of the fluorescein or cyanine-3 (Cy3) signal; detection by using a mouse anti-fluorescein antibody followed by a Cy3-labeled goat anti-mouse antibody; or resonance light scattering (RLS) detection by using streptavidin-coated gold particles. The dynamic range of representative PNA sequences suggests a fairly homogeneous window of detection of two log units of concentration, with the direct fluorescein isothiocyanate (FITC) detection being the least sensitive method (Figure 2 and Table 1)

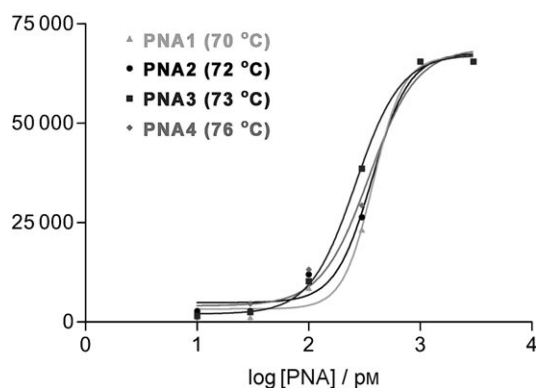


**Figure 2.** Fluorescence intensity versus concentration for the hybridization of four representative Cy3-labeled PNAs with  $T_m$  values ranging from 70–76 °C (in brackets). PNA1: GGAA TGG GTG CGAA; PNA2: AAGG GCA AGC; PNA3: GCCG CGA CGA GACG; PNA4: CGGC GGC ACG AGGC.

**Table 1.** Comparison of calculated  $EC_{50}$  values with the four different detection methods for PNA1.

	Detection method log concentration [ $\mu$ M]			
	Direct FITC scan	Antibody-amplified FITC scan	Direct Cy3 scan	RLS detection
$\log EC_{50}$	$3.457 \pm 0.127$	$2.072 \pm 0.155$	$2.578 \pm 0.069$	$2.457 \pm 0.092$
$R^2$	0.9542	0.9997	0.903	0.953

and resonance light scattering and antibody amplification of FITC being the most sensitive methods (10  $\mu$ M detection). Nevertheless, direct detection of Cy3-labeled libraries was found to be the best compromise between sensitivity and practicality as

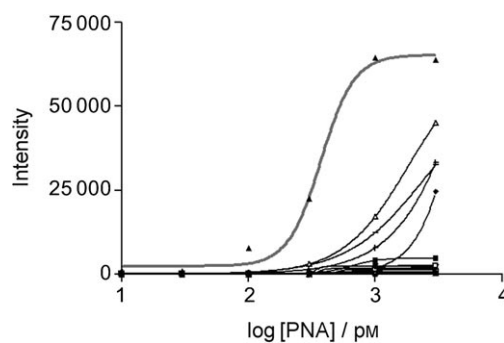


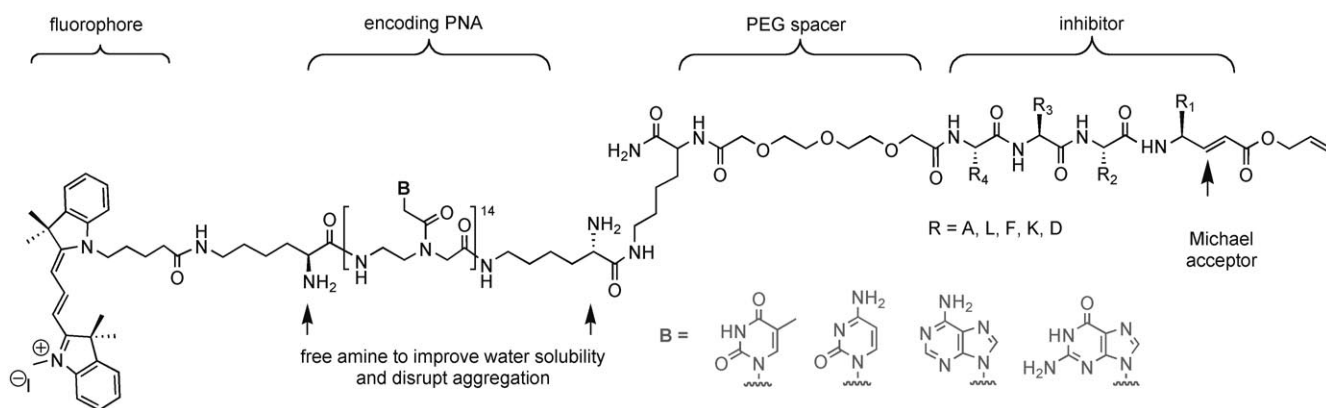
**Figure 3.** Fidelity of the hybridization. The intensity of the perfect match sequence for PNA3 (GCCG CGA CGA GACG) is shown as  $\blacktriangle$  and the next 20 most intense signals are shown in black.

it can be scanned directly after hybridization. Furthermore, it was observed that a Cy3-labeled library appeared more soluble than an FITC-labeled one. With respect to the fidelity of hybridization, the perfect match hybridization at 50% intensity was always at least five times more intense than the second brightest signal from a mismatched sequence for the sequences tested (Figure 3).

#### Gel-based selection of protein-bound compounds

An important advantage of PNA-encoded libraries compared to microarrayed libraries is that they can be used in solution prior to the read out by hybridization. For screening purposes, this allows for a selection of compounds bound to a protein prior to hybridization, which means that a screen can be carried out on orphan proteins for which there are no known ligands or substrates. We have previously demonstrated that size-exclusion filtration can be used to separate PNA-encoded compounds bound to a protein from unbound compounds in crude extracts. We now report a more focused approach based on gel separation, which was applied to cathepsin K as well as cathepsin F, a more recently identified member of the cathepsin family for which the preferred substrate has not been defined.

Cathepsin K is a lysosomal cysteine protease expressed predominantly in osteoclasts and has been associated with the degradation of bone matrix and bone resorption. Individuals bearing a dysfunctional mutant of cathepsin K suffer from a rare skeletal growth deformation.<sup>[12]</sup> Knock-out mice lacking cathepsin K were shown to be osteopetrotic, which makes cathepsin K a potential target for therapy against diseases such as osteoporosis.<sup>[13–15]</sup> Recombinant cathepsin K was incubated with a 625-compound library targeting cysteine protease with an acrylate functionality (Scheme 1). The library contains all permutations of the tetrapeptide, with small hydrophobic, large hydrophobic, aromatic, basic, and acidic residues. After 5 h, the mixture was loaded on a gel and separated; the band corresponding to the cathepsin K-inhibitor adduct was then cut from the gel. The cathepsin K-inhibitor complex was then removed from the gel slab by electroelution. As expected, there is a difference in migration between cathepsin K alone



**Scheme 1.** Chemical structure of PNA-encoded cysteine protease inhibitor library.

and the cathepsin K–PNA–inhibitor adduct (Figure 4, lane 1 versus lane 2). As a control, cathepsin K was preincubated with a generic suicide cysteine protease inhibitor (E64) prior to ad-

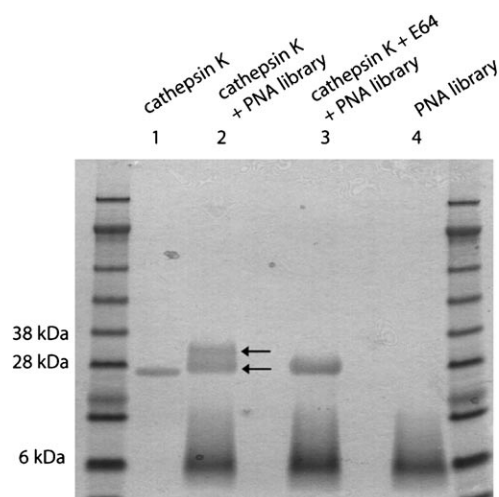


**Figure 4.** SDS-PAGE separation of the inhibitor–enzyme complex. Activated and E64-inhibited cathepsin K was incubated with a 625-member library of PNA-encoded inhibitors and separated on a 4–12% SDS PAGE gel. Lane 1: cathepsin K alone; lane 2: cathepsin K incubated with an inhibitor library; lane 3: E64-treated cathepsin K; lane 4: inhibitor library alone. See the text for details.

dition of the library. As anticipated, there is no band corresponding to the cathepsin K–inhibitor visible on the gel (Figure 4, lane 3). The selected inhibitors bound to cathepsin K were isolated from the gel by electroelution and hybridized to the microarray (Figure 5A and E).

The hybridization results point to Lys–Lys–Leu–Phe (KKLF, written N to C terminus) being a preferentially selected inhibitor due to its high spot intensity. Importantly the band corresponding to the acrylate library alone or to cathepsin K preinactivated with E64 showed no signal for the corresponding spot (Figure 5C and D). To determine the efficacy of the inhibitors identified by the hybridized array, some of these compounds were resynthesized individually without the PNA tag

and tested for their ability to inhibit cathepsin K activity in vitro.

Additionally, several inhibitors that showed weak intensity, Asp–Lys–Leu–Asp (DKLD) and Lys–Lys–Phe–Phe (KKFF), were synthesized and tested to determine their inhibition of cathepsin K activity (Table 2). The most active inhibitor found through this screen was KKLF with an inactivation rate constant of  $2528.7 \pm 99.6 \mu\text{s}^{-1}$ , while a control compound with weak intensity on the microarray (DKLD) showed poor inhibition (inactivation rate constant =  $16.3 \pm 4.1 \mu\text{s}^{-1}$ ). It is known that the main determinant of cathepsin K selectivity is the residue at P2 (the second amino acid position from the scissile bond) with proline being the preferred amino acid.<sup>[16]</sup> While proline was not used in the present library, the selected inhibitors have a very strong preference for leucine at P2. A recent study implicates cathepsin K in the cleavage activation of tartrate-resistant acid phosphatase (TRAP), a metallophosphoesterase that is associated with bone resorption.<sup>[17]</sup> Upon sequence inspection of the cleaved loop of TRAP, it is evident that the P2 sites contain leucine residues (Leu142 and Leu159) and the results obtained from the microarray profile are physiologically relevant.

Cathepsin F, another lysosomal cysteine protease closely related to cathepsin K, has recently been implicated in atherogenesis.<sup>[18]</sup> Indeed, there is strong evidence that cathepsin F secreted by macrophages is one of the few proteases responsible for the degradation of low-density lipoprotein that results in the generation and accumulation of extracellular lipid droplets in the arterial intima, a key feature of atherogenesis. To date, the preferred substrate selectivity of cathepsin F has not been reported. To determine if the PNA-profiling method presented here could identify inhibitor(s) that are specific for cathepsin F over cathepsin K, we profiled cathepsin F (Figure 5B and F). As with cathepsin K, incubation of the PNA-encoded acrylate library with cathepsin F resulted in a gel shift for the cathepsin F inhibitor, which was then isolated by electroelution of the gel slab (see Figure 3 in the Supporting Information). The sample was then hybridized to obtain the profile of preferred inhibitor substrates for cathepsin F, with a strong preference shown for Lys–Leu–Leu–Leu (KLLL, written N to C terminus). The inhibitor with this sequence was resynthesized without the PNA tag and the inhibition of cathepsin F was deter-

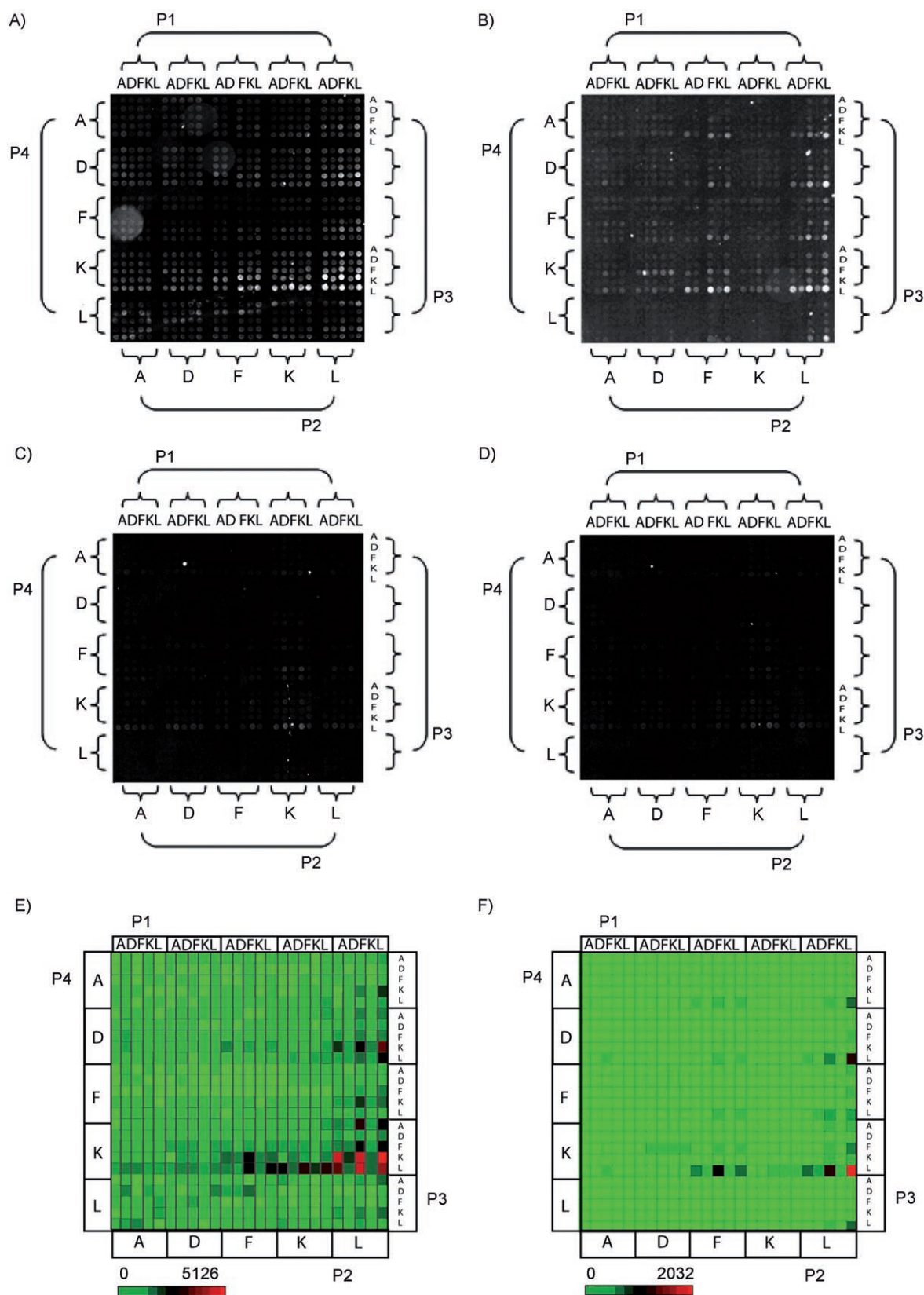


**Figure 5.** Hybridization of Cy3-labeled captured PNA probes isolated from a gel to a Schott slide array. A) Hybridization of sample of cathepsin K plus the acrylate library; B) hybridization of cathepsin F plus the acrylate library; C) acrylate library alone; D) hybridization of E64-treated cathepsin K plus the acrylate library; E) heat-map representation of the integrated signals in (A) for cathepsin K; F) heat-map representation of the integrated signals in (B) for cathepsin F. See the text for details.

**Table 2.** Pseudo first-order inhibition rate constant ( $k_{\text{inact}}$ ) for selected inhibitor probes and their corresponding spot intensities from hybridized arrays with the acrylate library incubated with cathepsins K and F.

Inhibitor sequence	Cathepsin K		Cathepsin F	
	$k_{\text{inact}}$ ( $1 \mu\text{s}^{-1}$ )	spot intensity	$k_{\text{inact}}$ ( $1 \mu\text{s}^{-1}$ )	spot intensity
DKLD	$16.3 \pm 4.1$	1067	$0 \pm \text{n/a}$	13
KKFF	$0 \pm \text{n/a}$	2705	$0 \pm \text{n/a}$	131
KKLF	$2528.7 \pm 99.6$	4751	$0 \pm \text{n/a}$	100.7
KLLL	$343.7 \pm 68.3$	4292	$2832.5 \pm 113$	2032

mined to be  $2832 \pm 4.1 \mu\text{s}^{-1}$  (Table 2). As with cathepsin K, there is a good correlation between the fluorescence intensity and the inhibition of the purified compounds. Importantly, despite the close relationship between cathepsin F and cathepsin K, the inhibition profiles of the two enzymes are clearly discernable with respect to their preference for K or L at the P3 position in the inhibitor. Indeed, the best inhibitor verified by enzymatic assays of cathepsin K (KKLF) shows no discernable inhibition of cathepsin F. Likewise, the best inhibitor for cathepsin F (KLLL) is not an effective cathepsin K inhibitor; it has approximately eightfold less inhibition for cathepsin K. These results are consistent with a recent report of the substrate-specificity profiles for several cathepsins determined by using fluorogenic substrate libraries.<sup>[19]</sup> Our results show that the microarray inhibitor screen is capable of providing selective protease inhibitors upon initial screening. In general, it is unlikely that proteases of interest are selective for a unique peptide substrate and having a profile of their activity is important in identifying inhibitors that will be able to discriminate amongst the tested proteases. It is important to note that in the case reported herein it is a change in two residues (P3 and P1) that confers the respective specificity between cathepsin F and K and this could not have been found with positional scanning libraries.

## Conclusion

We have developed a new selection method for the separation of protein-bound PNA-encoded molecules from solution-based library members. We have also developed and validated a new codon system and optimized a method for generating self-assembled small-molecule microarrays that provides the flexibility required for it to be implemented in diverse laboratory settings. The described method was used to screen a targeted library against two therapeutically relevant cysteine proteases, cathepsin K and cathepsin F, for which orthogonal inhibitors had not previously been reported. The microarray results showed a difference in the selectivity of these closely related enzymes and led to the identification of specific inhibitors. Finally, the gel-based isolation of selected inhibitors described herein adds to the repertoire of functional techniques to screen PNA-encoded libraries.

## Experimental Section

**Spotting of oligonucleotides from SCC buffer:** Corning UltraGAPS aminosilane-coated slides ( $25 \times 75 \text{ mm}$ , Corning Inc., NY) were used for all experiments. Typically, 20 slides were loaded into a GeneMachines Omnigrid Accent microarray printer equipped with 4 ArrayIT brand pins for contact printing. Oligonucleotides ( $1 \text{ mg mL}^{-1}$  in  $3 \times \text{SSC}$ ) were printed with a spacing of  $200 \mu\text{m}$ , and 12 complete arrays were printed per slide. Printing was performed at 75% relative humidity and  $20^\circ\text{C}$ . Slides dried immediately upon removal from the 75% relative humidity atmosphere and were rehydrated and "snap-dried" as follows. Slides were suspended array-side down over a water bath at  $80^\circ\text{C}$  for 5 s and then "snap-dried" by placing the slides array-side up on a hot plate at  $100^\circ\text{C}$  for 10 s. After cooling, the slides were crosslinked in a Stratalinker model 1800 UV crosslinker (Stratagene Corp) with 600 mJ of energy. Rehydrated and crosslinked slides were blocked for 1 h in a solution of  $100 \mu\text{g mL}^{-1}$  herring sperm DNA and  $0.22 \mu\text{m}$ -filtered blocker casein in phosphate-buffered saline (PBS; Pierce, Rockford, IL). Slides were then rinsed  $2 \times$  in  $18 \text{ M}\Omega$  water, spun dry, and stored in a desiccator until used.

**Spotting of oligonucleotides from DMSO:** All the oligonucleotides (amino-modified or not) were diluted to a final concentration of  $100 \mu\text{M}$  in 50% DMSO. The oligonucleotides ( $3 \mu\text{L}$ ) were transferred to a 1536-well spotting plate (Greiner) by using a Beckman Biomek 2000 pipetting robot (with BioArchimed software, TDZ ingenierie) according to a particular organization of the oligonucleotides on the plate to facilitate the analysis of the future array. The oligonucleotides were spotted in duplicate on aminosilane-coated slides (UltraGaps, Corning; A + MPX16 multiplex slides, Schott Nexterion) and on hydrogel-coated slides (H Schott Nexterion) by using a Microgrid II arrayer (Genomic Solutions) at 40–45% relative humidity and  $19\text{--}21^\circ\text{C}$ . After spotting, aminosilane-coated slides were dried for 48 h in a desiccator before crosslinking with UV at 600 mJ (Stratalinker, Stratagene) and hydrogel-coated slides were incubated in a chamber maintained at 75% relative humidity for 2 h.

**Hybridization of sample to DNA microarray:** Each sample consisted of probe ( $200 \mu\text{L}$ ; Cy3-, FITC-, or biotin-labeled) in hybridization solution containing 1% casein, PBS, and 40% formamide. Sample ( $40 \mu\text{L}$ ) was added to each of the four subarrays that made up a 625-member codon array. The sample holder was spun at 1500 rpm for 10 s and incubated for 18 h at  $50^\circ\text{C}$  with shaking at 1150 rpm in an iEMS Incubator/Shaker (Thermo Electron Corporation). The sample solution was then removed by centrifugation at 2000 rpm for 10 s. Fresh hybridization solution ( $40 \mu\text{L}$ ) was added to each subarray and the mixture was incubated at  $25^\circ\text{C}$  for an additional 10 min; the process was repeated and followed by an automated Tecan wash step with a solution of PBS and 0.005% Tween 20. The sample holder was then spun dry by centrifugation at 2000 rpm for 10 s at which point it was ready for further processing according to the signal detection method (either fluorescence or RLS).

**Detection of fluorescein- and Cy3-labeled probes hybridized to a DNA microarray:** The washed sample holder was disassembled and the hybridized slide was placed in a 50-mL conical tube where it was washed twice with deionized water. The slide was then spun dry by centrifugation at 2000 rpm for 10 s. The array was then read in an ArrayWoRx scanner (Applied Precision) at  $10 \mu\text{m}$  resolution by using FITC or Cy3 filters with a 0.4-s constant exposure time. The array image was analyzed with ArrayVision software (Imagine Research Inc.).

**Detection of biotin by RLS:** A prehybridization solution (20  $\mu\text{L}$ ; 1% casein, PBS, and 100  $\mu\text{g mL}^{-1}$  herring sperm DNA) was added to each subarray on a hybridized slide prepared as described above and the slides were incubated at room temperature for 10 min. The solution was removed by centrifugation at 2000 rpm for 10 s, and this was followed by addition of RLS particle solution (20  $\mu\text{L}$ ; 1% casein, PBS, 250 mM NaCl, goat immunoglobulin G (IgG), and streptavidin-functionalized gold nanoparticles). The binding process for the RLS particles consisted of incubation at 20 °C for 1 h with shaking at 2000 rpm. After incubation, the slide holder was washed by using Tecan as described earlier and spun dry by centrifugation at 2000 rpm for 10 s. The slide holder was disassembled and the slides were rinsed twice with deionized water. The slides were spun dry by centrifugation at 2000 rpm for 10 s and dipped in archiving solution, then the excess archiving solution was removed by centrifugation. The slides were scanned by using a Genicon RLS detection and imaging system (Invitrogen Life Sciences). The scanned arrays were analyzed with ArrayVision software.

**Automated hybridization by using a Discovery (Ventana Medical) system:** The following solutions were used: a blocking solution prepared with formamide (50 mL), 20 $\times$  SSC (25 mL), milliQ water (22 mL), 5% bovine serum albumin (BSA; 2 mL), and 20% SDS (1 mL); hybridization buffers (28% or a 40% final formamide concentration) commercially available from Ventana; and a manual washing buffer made with 0.1% SDS and 2 $\times$  SSC in water. The PNAs were dissolved in deionized water at 100 $\times$  their final concentration and this solution (2  $\mu\text{L}$ ) was then added to the Ventana hybridization buffer (200  $\mu\text{L}$ ). This solution was heated to 100 °C for 1 min and then centrifuged (20000g, 1 min) immediately before hybridization. The microarrays were first incubated in the blocking solution at 42 °C for 1 h in a coplin jar, washed with 3 consecutive milliQ water baths, then dried by centrifugation (1500 rpm, 2 min). The arrays were then introduced into the Ventana Discovery machine, the PNA solutions were added, and the hybridization was carried out for 8 h at 50 °C with agitation. The hybridization solution was removed and the slides were washed and developed with the antibody solution according to the manufacturer's protocol. Briefly, the arrays were washed with Ventana Ribowash (2 $\times$ ), the primary antibody (mouse anti-FITC, Ventana, 1 mg mL $^{-1}$  diluted 100 times in Ribowash) was added, and the arrays were incubated for 20 min at 37 °C. The arrays were washed with Ribowash (2 $\times$  at 23 °C), the secondary antibody (goat anti-mouse IgG, Jackson Immunoresearch 115-166-071, 1 mg mL $^{-1}$  diluted 100 times in Ribowash) was added, and the arrays were incubated for 20 min at 37 °C. The arrays were washed with a last cycle with Ribowash, then removed from the Ventana machine and washed manually by rapid dips in the washing buffer (once) and then in deionized water (twice). The slides were dried by centrifugation (1500 rpm, 2 min), scanned on a Perkin-Elmer ScanArray 4000 scanner at 100% laser intensity and 80% photomultiplier tube. The slides were quantified with Image 5.1 software (BioDiscovery).

**Isolation of enzyme-bound PNA-encoded inhibitors:** Recombinant human cathepsin K was prepared and purified as described previously.<sup>[14]</sup> Cathepsin K at a concentration of 5  $\mu\text{M}$  was incubated with a 625-member PNA-encoded inhibitor library with a total probe concentration of 96  $\mu\text{M}$  for 5 h at 37 °C. The samples were then spun in an Eppendorf 5417R centrifuge at 20817 relative centrifugal force for 10 min to pellet out any precipitated probe. The soluble fraction was then made up to 5 mL in lysosomal cysteine protease buffer (LCPB) consisting of sodium acetate buffer

(100 mM, pH 5.5), ethylenediaminetetraacetate (EDTA, 1 mM), dithiothreitol (DTT, 5 mM), and 0.01% Brij 35. The sample was then concentrated by using an iCON centrifugal filtration device (Pierce) with a molecular weight cut-off (MWCO) of 20 kDa and separated on a NuPAGE 4–12% SDS PAGE gel (Invitrogen) with  $\beta$ -morpholinoethanesulfonic acid (MES) buffer. The gel was then stained with Gel Code Blue Stain (Pierce) according to the manufacturer's instructions. Upon visualization of the inhibitor-tagged protease, the band was cut out and the gel sample was placed in a D-Tube dialyzer minidialysis device with an MWCO of 12–14 kDa (Novagen). The sample was then placed in an electrophoresis chamber and a constant current of 100 V was applied for 1 h in order to electroelute the sample from the gel. The recovered sample was then diluted in hybridization buffer and applied to a microarray device for analysis.

**Cathepsin K and F activity assays:** Cathepsin K and F protease activities were monitored at 37 °C by using a SpectraMax Gemini XPS fluorescence plate reader at an excitation wavelength of 380 nm and with an emission wavelength of 450 nm. Inactivation progress curves were carried out by using constant concentrations of enzyme at 0.1 nM in LCPB. A 10 min incubation with the substrate Z-Leu-Arg-MCA (Z = benzyloxycarbonyl, MCA = methylcoumarin acetamido; 80  $\mu\text{M}$ , Peptide Institute Inc.) was carried out at room temperature prior to the addition of varying concentrations of inhibitors. Inhibitors were prepared in DMSO and the final concentration of DMSO was 0.3%.

**Determination of inactivation rate constants:** The kinetic traces from cathepsin K activity assays (monitored with a latent fluorescent peptide substrate) were analyzed by using the software DynaFit.<sup>[20]</sup> For each inhibitor listed in Table, eight kinetic traces at various inhibitor concentrations ( $[I]_0 = 0, 10, 20, \dots, 70 \mu\text{M}$ ) were combined in a global analysis mode.<sup>[21]</sup> The initial enzyme concentration ( $[E]_0 = 0.1 \text{ nM}$ ) was treated as a locally optimized model parameter, within 5% titration error, in all except the control data set ( $[I]_0 = 0$ ). The mathematical model automatically derived by DynaFit is represented by the first-order ordinary differential equation system, represented by Equations (1a)–(1f) ( $[ES]$ ,  $[P]$ , and  $[EI]$  = the concentrations of the enzyme–substrate complex, product and enzyme–inhibitor complex, respectively). The enzyme–substrate association rate constant  $k_1$  was assumed to have a diffusion-controlled value of  $10^7 \text{ M}^{-1} \text{ s}^{-1}$ .<sup>[22]</sup> The substrate kinetic constants  $k_2$  and  $k_3$  were derived from the independently determined steady-state parameters  $K_m = (k_2 + k_3)/k_1$  and  $k_{\text{cat}} = k_3$  ( $K_m$  = the Michaelis constant,  $k_{\text{cat}}$  = the rate constant of catalysis).

$$d[E]/dt = -k_1[E][S] + (k_2 + k_3)[ES] - k_{\text{inact}}[E][I] \quad (1a)$$

$$d[S]/dt = -k_1[E][S] + k_2[ES] \quad (1b)$$

$$d[ES]/dt = k_1[E][S] - (k_2 + k_3)[ES] \quad (1c)$$

$$d[P]/dt = k_3[ES] \quad (1d)$$

$$d[I]/dt = -k_{\text{inact}}[E][I] \quad (1e)$$

$$d[EI]/dt = k_{\text{inact}}[E][I] \quad (1f)$$

For each kinetic trace, the mathematical model for the observed fluorescence intensity was computed as  $F_{\text{obs}}(t) = F_0 + \varepsilon_p[P](t)$ , where  $F_0$  is a locally optimized offset,  $\varepsilon_p$  is a globally optimized molar re-

sponse coefficient, and  $[P](t)$  is the time-dependent concentration of the reaction product P.

**E64 inactivation of cathepsin K:** Cathepsin K was inactivated by incubation with an irreversible cysteine protease inhibitor E64 (Sigma–Aldrich). Briefly, cathepsin K in LCPB at a concentration of  $5\ \mu\text{M}$  was incubated with  $28\ \mu\text{M}$  E64 for 30 min at  $37^\circ\text{C}$  and in the absence of substrate. Complete inhibition of enzymatic activity was verified by using the fluorescence-based activity assay described above.

## Acknowledgements

A fellowship from the Region d'Alsace (FD.) is gratefully acknowledged. This work was supported in part by grants from the Human Frontier Science Program (HFSP 0080/2003) and the European Commission (MIRG-CT-2004-505317).

**Keywords:** combinatorial chemistry · microarrays · nucleic acids · proteases · proteomics

- [1] M. Uttamchandani, D. P. Walsh, S. Q. Yao, Y.-T. Chang, *Curr. Opin. Chem. Biol.* **2005**, *9*, 4.
- [2] D. Barnes-Seeman, S. B. Park, A. N. Koehler, S. L. Schreiber, *Angew. Chem.* **2003**, *115*, 2478; *Angew. Chem. Int. Ed.* **2003**, *42*, 2376.
- [3] F. G. Kuruvilla, A. F. Shamji, S. M. Sternson, P. J. Hergenrother, S. L. Schreiber, *Nature* **2002**, *416*, 653.
- [4] C. M. Salisbury, D. J. Maly, J. A. Ellman, *J. Am. Chem. Soc.* **2002**, *124*, 14868.
- [5] Q. Zhu, M. Uttamchandani, D. Li, M. L. Lesaichere, S. Q. Yao, *Org. Lett.* **2003**, *5*, 1257.
- [6] M. Schutkowski, U. Reimer, S. Panse, L. Dong, J. M. Lizcano, D. R. Alessi, J. Schneider-Mergener, *Angew. Chem.* **2004**, *116*, 2725; *Angew. Chem. Int. Ed.* **2004**, *43*, 2671.
- [7] J. Harris, D. E. Mason, J. Li, K. W. Burdick, B. J. Backes, T. Chen, A. Shipway, G. Van Heeke, L. Gough, A. Ghaemmaghami, F. Shakib, F. Debaene, N. Winssinger, *Chem. Biol.* **2004**, *11*, 1361.
- [8] N. Winssinger, R. Damoiseaux, D. C. Tully, B. H. Geierstanger, K. Burdick, J. L. Harris, *Chem. Biol.* **2004**, *11*, 1351.
- [9] J. L. Harris, N. Winssinger, *Chem. Eur. J.* **2005**, *11*, 6792.
- [10] G. Abbenante, D. P. Fairlie, *Med. Chem.* **2005**, *1*, 71.
- [11] U. Giesen, W. Kleider, C. Berding, A. Geiger, H. Orum, P. E. Nielsen, *Nucleic Acids Res.* **1998**, *26*, 5004.
- [12] B. D. Gelb, G. P. Shi, H. A. Chapman, R. J. Desnick, *Science* **1996**, *273*, 1236.
- [13] U. Grabowski, T. J. Chambers, M. Shiroo, *Curr. Opin. Drug Discovery Dev.* **2005**, *8*, 619.
- [14] D. N. Deaton, A. M. Hassell, R. B. McFadyen, A. B. Miller, L. R. Miller, L. M. Shewchuk, F. X. Tavares, D. H. Willard, L. L. Wright, *Bioorg. Med. Chem. Lett.* **2005**, *15*, 1815.
- [15] D. G. Barrett, V. M. Boncek, J. G. Catalano, D. N. Deaton, A. M. Hassell, C. H. Jurgensen, S. T. Long, R. B. McFadyen, A. B. Miller, L. R. Miller, J. A. Payne, J. A. Ray, V. Samano, L. M. Shewchuk, F. X. Tavares, K. J. Wells-Knecht, D. H. Willard, Jr., L. L. Wright, H. Q. Zhou, *Bioorg. Med. Chem. Lett.* **2005**, *15*, 3540.
- [16] F. Lecaille, Y. Choe, W. Brandt, Z. Li, C. S. Craik, D. Broemme, *Biochemistry* **2002**, *41*, 8447.
- [17] J. Ljusberg, Y. Wang, P. Lang, M. Norgard, R. Dodds, K. Hultenby, B. Ek-Rylander, G. Andersson, *J. Biol. Chem.* **2005**, *280*, 28370.
- [18] M. Sneek, P. T. Kovanen, K. Oorni, *J. Biol. Chem.* **2005**, *280*, 37449.
- [19] Y. Choe, F. Leonetti, D. C. Greenbaum, F. Lecaille, M. Bogyo, D. Bromme, J. A. Ellman, C. S. Craik, *J. Biol. Chem.* **2006**, *281*, 12824.
- [20] P. Kuzmic, *Anal. Biochem.* **1996**, *237*, 260.
- [21] J. M. Beechem, *Methods Enzymol.* **1992**, *210*, 37.
- [22] T. E. Creighton, *Proteins: Structure and Molecular Properties*, 2nd ed., W. H. Freeman, San Francisco, **1992**.

Received: June 8, 2006

Published online on September 28, 2006

**CHEMBIOCHEM**

## Supporting Information

© Copyright Wiley-VCH Verlag GmbH & Co. KGaA, 69451 Weinheim, 2006

# CHEM**BIO**CHEM

## Supporting Information

for

### Self-Assembled Small Molecule Microarrays for Protease Screening and Profiling

Hugo D. Urbina, François Debaene, Bernard Jost, Christine Bole-Feysot,  
Daniel E. Mason, Petr Kuzmic, Jennifer L. Harris, and Nicolas Winssinger\*

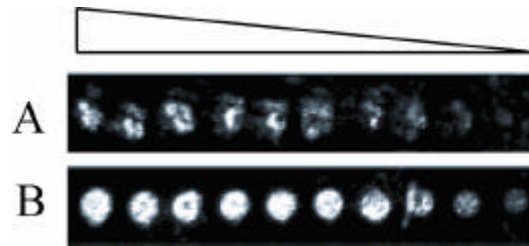


**Figure S1.** Printing oligos in A) 50% DMSO and B) 3X SSC and optimization of printing concentrations. Concentration of spotted 25-mer oligos range from 0.1 through 0.01 mg mL<sup>-1</sup>.

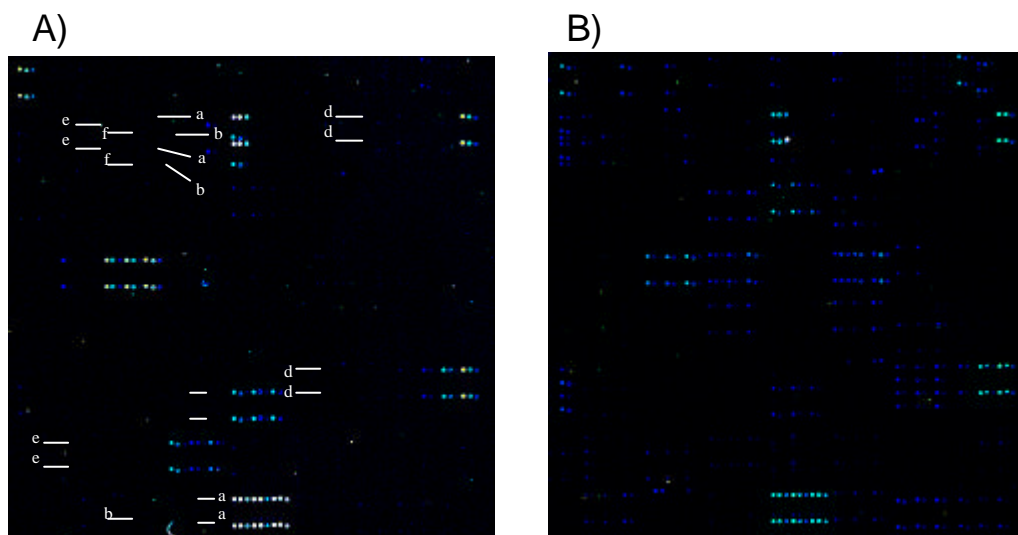


**Figure S2.** Visualization of 6 PNA sequences hybridization (1 nM per probe), depending on their  $T_m$  and the formamide concentration on hybridization solution. Target oligonucleotides were spotted in duplicate as described in the methods. Both hybridization were done at 52 °C, with either A) 50 % formamide or B) 28 % formamide under the same buffer system. a: GGGTGACGTCGGGA  $T_m=73$  °C; b: CCGTGATACATGAAA  $T_m=58$  °C; c: GGCTCTACGGGCAA  $T_m=66$  °C; d: GGGTAGAAAGAAGG  $T_m=67$  °C; e: CCGTCGAGCCTAAG  $T_m=62$  °C; f: GGCTACAGTGAGAC  $T_m=62$  °C

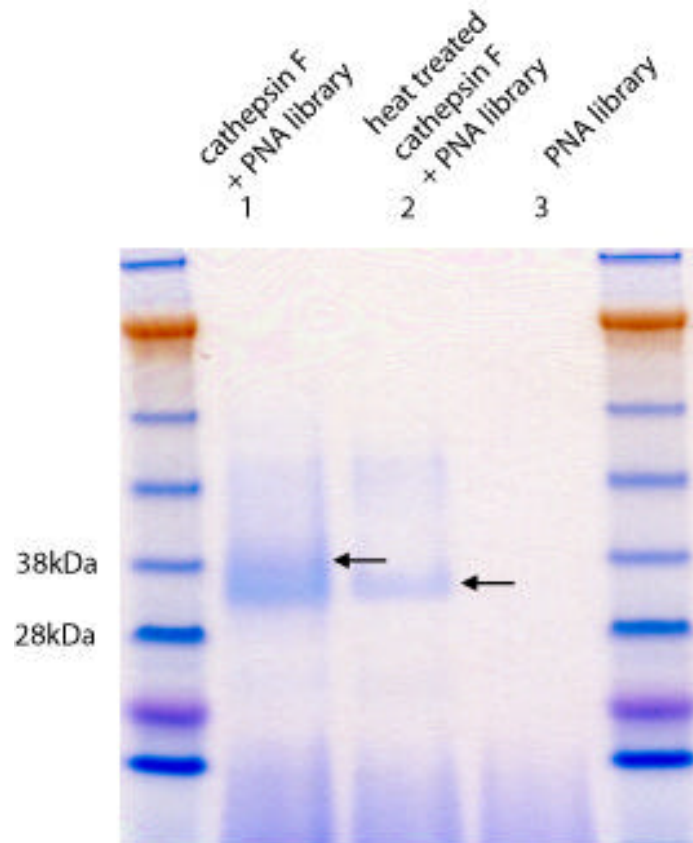


**Figure S3.** Lane 1, cathepsin F incubated with PNA library; Lane 2, cathepsin F heat treated (90°C for 5 min) before addition of PNA library; lane 3, PNA library alone. Arrows indicate where the gel slabs were excised from the gel. See text for details

**Table S1.** Integration of fluorescent intensity from figure 3.

cathepsin K + acrylate library		E64 treated cathepsin k plus acrylate library		acrylate library alone	
Inhibitor Probe	Intensity	Inhibitor Probe	Intensity	Inhibitor Probe	Intensity
KKLL	5126.226	KLKK	803.619	KLKD	981.347
KKLF	4751.114	KLKD	750.406	KLKK	927.730
KKLA	4694.016	KLLD	518.669	FKKD	657.579
KLLF	4467.938	FKKK	447.708	FKKK	633.135
KLLL	4292.590	FKKD	436.382	KLKA	577.180
KLLA	3566.195	KLKL	432.289	KLDD	531.724
DKLL	3537.750	KDKD	422.726	KLAD	511.539
KALF	3155.828	KLKA	378.193	AKDF	503.779
KLKF	3139.050	KKKL	320.072	KLAA	488.554
KLKL	3133.154	ALKD	317.666	KLKF	481.560
KALL	2871.375	FLKK	303.783	KDKD	457.000
DKLF	2814.819	ALKK	300.652	FLKK	440.810
KKFF	2705.718	KLLA	299.887	KLLD	439.585
KLKA	2691.571	KLFD	292.290	FLKD	438.639
KLFF	2533.787	KLKF	285.254	KLDK	430.394
KFLL	2516.911	KDKK	282.802	KLDA	402.063
KLFL	2355.081	FLKD	282.256	KLAK	401.575
KFLF	2308.243	KDFK	279.250	KLKL	384.789
DLLL	2275.164	KLAK	269.830	KLDF	377.063
KKLD	2166.922	FKLD	266.712	KLKF	375.631
KLKK	2084.329	KLDD	264.302	KLFD	355.245
AKLL	2045.067	KLLK	263.692	KLDL	353.133
DKLA	1871.299	KLKF	248.246	KDFK	351.140
FKLF	1850.557	KLLF	246.848	ALKD	343.453
KKFL	1783.245	FKLK	243.925	KLAF	338.327
KLKD	1751.621	KLDK	238.109	KDKK	335.151
LALL	1722.916	KKKF	231.340	FLAK	326.737
FKLL	1716.440	KDFD	208.229	ALKK	319.743
KLLD	1630.152	KKKD	207.756	KLLA	314.049
KKFA	1608.774	KDDK	202.618	FKLK	312.147
DLLF	1573.602	ALAD	202.057	ALAD	297.469
KKLK	1556.073	KFKL	201.900	KLLK	297.095
LKLL	1542.924	KFKA	198.553	KLFA	295.850
KLLK	1520.872	KFKD	197.545	KKKL	293.061
LDFF	1516.499	KDDD	196.383	FKLD	288.082
KDLL	1481.053	KKFK	189.618	KDAK	283.398
DFLL	1449.763	ALAK	189.477	FKKF	281.741
DALL	1448.443	ALLD	180.585	KLFF	278.510
KLFA	1422.675	KKLF	174.981	FLAD	278.265
DALF	1405.616	KDKA	171.733	KFKD	271.153
KFLA	1392.491	KFFK	170.522	KLFL	263.026
AKLF	1389.316	KLFL	169.029	KDFD	258.333
FFLL	1382.540	FKKA	164.244	KFKA	257.977
KKFK	1379.863	KDKF	162.628	KKKD	249.680

KALA	1376.572	KKFL	162.528	KDDK	242.640
KKFD	1371.412	FLAD	161.780	KDAD	241.740
KLDD	1341.038	FLLD	158.129	FKKA	241.514
KLFK	1335.961	KLDL	157.953	KLAL	238.589
KKKL	1330.719	KKLD	153.169	KKKF	238.343
KKKD	1303.953	FKDD	152.298	ALKA	229.423
LDAD	1298.136	ALKL	151.334	KLLF	226.823
KLDL	1270.196	KKKA	150.642	FKDK	225.059
LDDL	1268.246	KFKF	149.199	KFFK	219.519
KLAD	1261.702	FLKL	149.119	KFKL	219.259
DFLF	1260.574	FKKL	149.079	ALAK	216.067
DKLK	1250.385	FKDK	148.634	FLFK	207.071
KLDF	1215.824	KKLA	147.909	FLKL	206.616
LLAF	1211.289	FKKF	147.624	FLFD	202.211
LKLF	1205.020	KAKD	147.483	FKAD	200.913
KLAF	1204.046	KAKL	147.180	ALKL	200.426
KFLD	1190.847	FLDD	146.205	FLFL	199.758
DKFA	1178.069	KLLL	140.274	KKFK	194.754
KLFD	1174.370	KLFA	139.093	FLDK	194.064
LAKA	1168.412	KLDA	138.312	ALLD	191.958
ALLL	1157.622	ALKA	137.391	KFFD	189.765
DKFL	1152.890	KLDF	134.489	KDKA	188.452
KAKL	1145.609	FKAD	133.719	KFKK	180.434
LLAD	1139.115	KAKA	133.375	KFKF	179.037
DLKL	1131.837	FLFD	128.386	KAKA	176.981
KFFF	1131.120	KFFL	127.104	FKKL	175.684
LFDF	1125.046	ADKD	125.294	KKLF	173.913
KFFA	1116.218	KDLD	124.587	KKFL	171.010
DAKL	1104.344	ALDK	123.549	KKLA	168.494
KLAL	1096.273	KFKK	122.639	KAKL	168.256
KFKL	1094.657	KFFD	122.598	KKDD	167.406
KKKF	1091.863	ALAL	122.090	KAKD	166.339
KFDA	1088.077	KALD	121.775	FLLD	165.922
KFFL	1081.846	KFLD	121.245	KDDD	165.814
KDLF	1081.128	KKKK	118.420	ALDK	162.883
KFKA	1080.372	FDAK	118.330	FDDK	157.994
DKFF	1080.327	FLFK	117.619	KDLK	157.397
KFDF	1073.889	KDLK	116.231	FDDD	156.235
KALD	1071.198	FLDK	115.972	KKKA	155.703
DKLD	1067.618	FKAK	112.917	ALDD	154.806
DLLA	1052.443	KLFF	109.873	ADKD	150.880
KLAK	1047.063	KKFD	108.757	FLKF	150.557
LALF	1032.450	FLFL	108.038	KKFD	150.437
KALK	1022.758	FAAK	107.297	FKAF	143.240
FLLF	1021.845	ALDD	105.911	ALKF	143.011
KFKD	1016.339	ALLK	104.759	ALAA	142.442
FKLK	1015.769	KLAL	104.349	LLKA	142.073
KLAA	1008.781	FDDK	104.069	KKLD	138.937
KLDA	1002.242	FDDD	102.497	KAKK	138.285
KKDD	1000.728	FLAK	101.118	KDKF	137.828

LLKA	992.163	KAKK	99.991	KFDD	137.570
DKAD	990.470	KKDD	99.665	FLKA	135.433
ALKL	982.988	KFDD	97.292	FAAK	135.279
KFDL	982.360	FLKF	96.683	FKAA	133.448
AALL	957.581	KKAF	92.639	KFFL	131.454
LDFD	948.949	FKAF	90.933	ALLK	129.136
KKDF	935.200	ALKF	89.470	ALAL	129.059
DKKL	932.661	FLKA	88.820	KFFA	127.606
FKLD	928.454	DKAD	87.881	FDAD	126.970
KKDL	925.816	KFDL	86.913	AFKD	125.895
LKLA	922.042	KKLL	86.003	ALFL	123.753
FKLA	920.728	AFKD	83.870	AKKD	122.758
KDLA	920.022	FKFL	83.172	FKFL	122.685
KLDK	919.606	KAFK	81.912	KDLD	121.211
KFDD	914.917	FLDL	81.637	FLLF	120.600
DLLK	912.761	AFKK	80.352	FDLK	119.614
LKAL	906.290	KAKF	80.053	KDFF	118.673
DLLD	906.020	FLLK	79.694	KKKK	118.653
KFLK	893.038	FKLF	76.700	KFDL	118.114
DDLL	891.968	FLAL	76.204	FDAK	116.646
DLKD	888.291	ALFD	75.481	FLAF	113.245
DFAD	885.942	DFAD	74.627	KDFA	110.507
KFKF	880.069	KAAD	74.427	FLAL	110.244
DFLA	879.959	ADKK	72.704	FLLK	109.777
LLLF	878.111	FDAD	71.681	KKDK	109.387
LDFA	872.249	AKAF	71.676	KKAF	108.322
DLKK	871.371	KFAF	70.866	KKDF	105.616
LFAL	861.263	FLLF	70.613	DKAD	104.410
DDLDF	860.377	KDFD	68.357	AKKF	103.393
LDAK	859.555	KKDK	67.996	KAAC	102.939
FLLF	859.530	KALA	67.662	KFLD	102.738
KKAD	842.316	KDFL	65.867	FKAK	101.638
KAKF	839.381	KKDF	65.746	KFDK	100.503
KKAL	837.426	KADD	65.148	KAAD	99.320
KKKA	837.017	KFFA	64.675	FKDD	99.190
LLAA	835.541	ALFL	64.001	AFKK	99.177
LAFL	835.283	ALFK	63.440	KKDL	98.525
ALLF	832.788	AKKD	63.380	FKDF	98.166
FKKD	827.678	KAAC	63.194	FAAD	97.196
LFDD	813.356	KADK	62.949	ALFD	96.411
DLFL	807.315	DFFD	62.341	FLFF	95.466
DLKF	802.916	FLDA	61.789	KFFF	95.235
DKKF	797.444	KFDK	61.328	LLFD	94.305
DALA	792.819	ALAA	61.247	FLDL	94.142
LLKL	788.176	KDFF	60.984	KFDA	94.049
FLLL	779.008	LKKD	60.657	LKKD	93.546
DAAD	778.911	KKLK	60.312	DFDD	93.439
KKDK	777.673	KKDL	59.840	KKLL	92.346
DFKL	775.793	ALDL	59.370	FKDA	91.872
KDLK	768.396	KDLF	59.185	KDFL	91.431

DKAF	764.289	KFFF	58.863	LLAD	89.006
LFL	760.321	FLL	58.788	KALD	88.472
DDKL	759.331	KDDL	58.253	ALFK	88.047
LLKF	758.315	FKDF	57.828	AKKL	86.297
FKFF	758.281	DLAF	57.488	KKFF	84.861
KAKD	754.864	KLAD	57.395	KAKF	84.766
ALKK	752.706	DKFD	56.987	LLDL	82.603
AFL	751.141	DKDD	56.961	FKLF	81.014
DLDD	748.193	KALK	56.634	KAFK	80.760
KDKD	738.351	KFDA	55.965	KKLK	79.933
KDAK	738.048	AKLF	55.889	AKLF	79.259
KFAD	731.509	LAKD	55.812	LKLA	76.941
KKAK	731.308	KAFD	55.181	KKAL	76.580
DLKA	730.766	AFKL	55.177	AKKK	75.930
FALF	729.968	DAKA	54.479	KDLF	75.247
LFLF	725.910	KAAL	53.981	FKFF	74.747
LKAK	723.452	KFLF	53.278	FDDA	74.461
KFFK	721.870	FDFD	53.174	KA AF	71.507
KFAL	721.415	FLAA	53.075	DKKF	70.846
DLDL	717.116	KKAD	52.215	KDDL	70.520
LLFL	712.889	KKAK	51.949	ALDA	70.080
KDFF	710.326	AFLD	51.926	DKKD	69.056
LKFF	709.976	FFKF	51.765	KLLL	68.563
KDKF	709.276	LAFD	51.395	KDFD	68.334
DLDA	707.254	FFKL	51.318	KKAD	67.710
FKKK	704.152	AAKD	51.190	ALDL	66.579
LDFK	698.773	KFAD	51.020	KFLK	66.317
KKAF	695.858	KFLA	50.399	KFAF	65.688
KKKK	695.841	LALD	49.712	DAKA	63.759
KFFD	690.298	LAKA	49.653	AKKA	62.471
DLAF	687.688	DFDA	49.173	KALA	61.738
AALF	685.061	KDFA	49.014	KAFD	61.421
LLFF	683.884	AKKL	48.950	FKAL	61.132
ALKD	683.524	KADA	48.815	FFKL	60.966
LFDK	683.258	KADL	48.603	KAFL	60.869
KADL	682.459	KKAL	48.138	FLAA	60.653
KFDK	678.787	DFDD	47.815	AKAF	60.622
LLLL	678.284	ALDA	47.332	KDAF	60.224
DLAD	673.157	AKDD	46.637	DKKA	59.840
KFAF	670.230	DADD	46.192	KDKL	58.828
KFAA	670.093	KFAA	45.650	ALFA	58.814
DLFF	669.447	KDKL	45.290	DKDD	58.754
AKFL	665.620	AAKK	45.160	ADKK	58.336
DFDA	665.581	AFDD	45.146	FDA A	56.735
KAFL	661.162	AKKK	45.099	DLAF	56.435
KAKA	660.644	FLDF	44.436	AFKL	56.306
LLKD	660.442	ADKL	44.377	DLFD	56.092
DDLA	658.382	LKKA	44.078	FAFD	55.619
DFLK	657.444	FKDA	44.023	FKDL	55.450
FLFL	655.776	FAAL	43.178	FLDF	55.444

LLDL	655.242	FKLL	42.651	KDAA	55.403
LALK	647.741	FAFD	42.536	FADA	55.346
LFDA	647.227	KFLL	42.402	AAKD	55.089
KFKK	646.141	DLAD	41.290	ALDF	54.023
FKAK	643.716	KDDA	40.947	KALF	52.955
DFAA	642.330	ADAK	40.605	AFKA	52.850
DLFA	641.316	DKAF	40.480	DAKD	52.557
FKFL	637.444	DAFD	40.478	KKAA	52.525
AKFF	636.372	DKFA	40.343	KALK	51.713
FDLL	634.911	ALFA	39.240	LLFK	51.598
KDLD	634.890	KAFL	37.849	DLAD	51.402
KKAA	634.019	AFDK	37.600	KFLL	50.821
AAKL	633.399	LLLD	37.494	LKLD	50.593
AFLF	630.324	LAKL	37.377	DADA	50.335
DKDL	627.857	DLFD	37.315	FFFD	50.209
FLKL	625.208	AKDF	37.213	AFLD	50.179
DAKF	624.744	DKKA	36.588	AAKK	50.087
KADF	623.546	FFFD	36.432	LAAD	49.951
FKKF	622.861	FKDL	36.431	FDAL	49.381
AADL	621.010	DLDD	36.399	DKKK	49.284
ALAD	618.626	DKDL	36.330	FFKD	48.863
KDFK	617.457	AFAK	36.321	LLAK	48.811
DKAA	617.447	KALF	35.972	ALFF	48.777
DFFD	616.501	KFAL	35.854	DKFA	48.751
LKFA	612.154	LDKD	35.710	FDDL	48.506
LKKL	608.940	KFLK	35.554	FDKL	48.366
ADLL	608.524	KDAK	35.250	AFDD	47.292
ALLD	606.570	DAKD	34.724	LKKK	47.233
DFFL	606.046	KAFA	34.583	DADD	47.206
LLFA	604.711	ADAD	34.494	AFKF	46.969
FKDF	604.694	FADA	33.845	ADAK	46.872
LLLA	602.309	KAAA	33.528	KAFA	46.717
LKLD	602.155	KKFF	33.054	AKDK	46.228
AKKL	595.766	FKAA	32.622	DKFD	46.221
DLAA	595.610	KALL	32.544	DKLF	46.141
DFAF	594.547	FDAA	32.463	FFKK	45.938
FLKD	592.422	FADL	32.047	DFAD	45.643
DKKA	591.912	AAKL	31.992	KKAK	45.606
DKDF	589.181	ALDF	31.793	KAAL	45.225
KADD	589.043	AKAK	31.586	DAFD	44.825
LKLK	588.486	DFAA	31.400	AKDD	44.237
DAKA	584.878	FDDA	31.105	KAAA	44.169
DADD	584.790	DKDA	30.198	LAKA	43.948
LKKD	583.805	DKDF	29.599	LKFF	43.682
DFLD	581.565	LKLD	29.269	FFAD	43.281
DFFA	580.489	DFKD	29.162	DKKL	43.234
DALK	578.681	AKAL	29.008	FADL	43.163
LLDF	578.556	FDDL	28.883	AAKL	42.592
FDAD	578.288	AFKF	28.879	DAAD	42.501
DADL	576.950	AFKA	28.825	DKAF	42.208

FLLD	576.810	ALAF	28.068	ADKA	42.181
AKLD	576.070	LDKF	28.023	KDDA	42.088
DLFD	575.820	DKLD	27.749	DDFA	41.889
FDLF	573.304	KLAA	27.597	LKLK	41.317
DKFD	573.039	ADKA	27.530	FKFK	41.294
ALFL	572.720	FLFF	27.471	KFAK	40.899
KDAD	572.246	DKAK	27.313	LAFD	40.472
LKFL	572.189	KDAA	27.249	ALLL	39.594
FLLK	571.875	DADA	26.495	LAKL	39.168
DKDA	571.654	DKLK	26.446	DDFF	38.691
AALA	570.113	ALLL	26.160	KADD	38.435
KAFA	569.876	FFFK	26.079	DDAD	38.309
KAFF	568.791	FLAF	25.957	DFKD	38.271
DDAD	568.214	LKKL	25.824	DKDK	38.207
KAAD	565.959	AKAD	25.519	KFAA	38.181
FLAF	565.619	DAAD	25.304	KFLF	37.833
FAKL	565.595	AAKF	25.211	LFLA	37.495
DKKD	563.907	DDAK	25.187	ADKF	37.210
KADA	560.722	ADKF	24.772	FLLL	36.754
KAFF	559.147	DFDK	24.592	ALAF	36.689
KFAK	558.630	DAKL	24.517	FDFF	36.137
FLKK	557.387	LAFD	24.455	DDLA	35.926
DLAL	556.851	KAFF	24.412	ADAD	35.907
DKAL	554.033	DAAK	23.492	FAAL	35.881
FLAD	553.412	DAAL	23.271	FFKF	35.652
KAKK	553.000	AKKF	23.231	AAAK	34.984
AADF	552.608	LFKA	23.155	ADKL	34.763
LKDL	550.153	LAFK	23.056	FKFD	34.712
ALKF	548.093	AKDK	22.805	ADDK	33.994
LADL	547.905	AKFD	22.746	DFAL	33.699
DLAK	542.423	LALA	22.472	LLKK	33.075
DKFK	538.907	KKFA	21.792	DAKF	32.991
DFKF	536.859	LKLK	21.494	LADD	32.888
DFDD	536.230	LAKK	21.415	LLLFF	32.400
KDFD	534.039	LDLF	21.186	KKFA	32.342
LFLA	529.572	ADLF	21.099	KFAD	32.258
DLFK	529.227	DDFA	21.093	DALA	32.049
DAAK	528.519	DKAL	21.073	ALLF	31.841
LFAA	524.982	KDLA	21.051	FFDL	30.904
DKAK	524.379	ADDK	20.833	DLDD	30.684
FKAD	522.301	AAAD	20.636	KFLA	30.433
LDAL	522.030	DKKF	20.247	AKLA	30.248
LDFL	518.185	KADF	20.178	AAKA	30.161
DAKD	518.024	DFAK	20.141	DLAA	30.157
KAFK	517.985	KDAL	19.865	KDLA	29.999
KDDA	517.250	DLDL	19.860	DFFF	29.910
FKAF	514.825	KAFF	19.742	KDLL	29.753
KDAF	513.206	DAFF	19.634	DFDA	29.747
LKKF	512.700	FFFK	19.615	FKFA	29.730
FFLA	511.033	KDLL	19.443	FFFK	29.681

LLLD	508.660	AADD	19.415	DAAF	29.543
ALKA	508.213	DFFA	19.378	DDDK	29.245
LDLL	508.086	AFFD	19.222	DADK	29.199
LLFD	507.276	DDDK	19.168	DAAK	29.189
LADF	506.663	AAAK	19.042	FFFL	29.148
LKFD	504.491	FDAL	18.840	KAFF	29.031
FLKF	504.370	DDFD	18.608	AFDK	28.938
FLLA	502.618	AKDA	18.552	DDKD	28.929
FFAK	502.370	FKFK	18.448	AAKF	28.794
KDKA	500.886	FFAD	18.273	FFAF	28.737
LKAD	500.719	DADK	18.271	KFAL	28.364
KDDD	500.020	LADD	17.795	FLDA	28.181
LFFF	499.698	LAFL	17.682	DFFD	28.181
FKDD	499.438	FKAL	17.649	KADK	28.119
ALDL	498.088	LDAL	17.519	FLLA	27.679
DFFF	496.041	FKFF	17.417	LFKL	27.636
LFDL	495.558	DKFL	17.230	FLFA	27.591
LAAD	495.300	DLDA	17.222	DAKL	27.355
FFLD	494.741	FAAD	17.019	KADA	27.017
AADD	494.209	LKLF	16.949	FALK	26.786
LAKL	493.970	DFDL	16.917	LDDA	26.780
LLKK	493.846	FFAL	16.723	LFLD	26.267
DADA	493.798	FFAK	16.709	LFFF	26.051
DDLK	492.331	FADD	16.553	DAKK	25.950
FKKL	490.776	ADDD	16.542	DKDL	25.851
AADA	488.804	DADF	16.510	DKAA	25.298
DADF	486.229	DAFA	16.435	DFDD	25.298
FLFF	484.786	FFAA	16.295	FDAF	25.118
AFKL	482.350	DLFA	16.278	LKDD	24.910
KDFL	481.382	LFFL	16.259	LKDK	24.616
ALLK	480.422	KDAF	15.945	ADFL	24.350
FLDD	480.368	DAAF	15.889	DAFA	24.317
DDFA	480.037	LFDF	15.577	DKLD	24.307
DDFL	479.263	KDAD	15.401	FDDF	24.065
DDAK	476.671	ADFL	15.398	LAKD	24.035
LKKA	475.956	DLLK	15.297	DDDD	23.903
AADK	475.314	DKAA	14.835	LADA	23.867
AAFF	474.798	LDAA	14.583	ADDD	23.573
FLDL	473.626	LALL	14.489	DAFF	23.505
LAKF	473.596	FKFD	14.440	FDFL	23.490
DKKK	472.613	DFKF	14.407	LDKL	23.363
ALFF	472.325	DFLK	14.014	DLAK	23.335
ALFA	470.831	DDFF	13.679	LAFL	23.127
LADK	469.165	DKKD	13.593	AADD	23.077
FKFA	467.046	AAAF	13.550	DADF	22.973
KADK	466.574	FFDL	13.507	FFDK	22.717
LADA	466.087	DADL	13.375	DADL	22.676
FALL	465.612	LFLF	13.349	LLFF	22.640
FAKD	463.198	DDDD	13.019	FADD	22.574
KAAC	460.657	ADAF	12.848	DDLD	22.548

LDDK	458.927	DKKK	12.757	FFDD	22.446
AKDF	455.739	DDAD	12.569	AKAK	22.225
DAKK	455.198	DAKF	12.552	DKFL	22.083
LKDF	454.165	FFFL	12.431	AALA	21.925
AFFF	453.717	DALD	12.257	LLAF	21.794
AKKF	453.525	FFLF	12.159	DLDL	21.617
LKFK	452.159	FALK	11.698	FALD	21.354
KAAL	450.718	ADDL	11.606	LKDA	21.111
KDFA	449.133	AFAD	11.598	FDFA	20.975
LALA	447.889	LFDL	11.344	LADF	20.815
AAFA	443.466	AAKA	11.146	FFFF	20.798
LAAK	443.231	FFAF	11.118	FKLL	20.722
KDKK	442.223	KKAA	10.806	AAAF	20.718
LLDD	439.957	AALF	10.558	DDFK	20.699
LAKD	439.255	AKLL	10.370	LFKK	20.609
AKAF	438.882	LDKK	10.336	AKDL	20.600
Lafa	438.662	DKDK	10.291	LLAL	20.498
AKFA	438.139	LKAL	10.256	AKFL	20.484
LDAA	437.907	FLFA	10.220	LKAF	20.271
ADLF	437.549	AALD	10.157	LFLF	20.054
KDDF	435.860	LFFF	10.057	FAAF	20.011
DDLD	435.759	LALK	9.989	DKDA	19.994
DAFL	434.937	LADL	9.960	AKAD	19.898
LLFK	434.688	FAAA	9.927	LFDA	19.324
FKDA	433.617	DFAF	9.904	LDFD	19.313
AKDL	430.437	FFFA	9.689	AFLK	19.295
FKKA	429.917	DDDL	9.663	Ldff	19.117
KDDK	429.881	DKLF	9.646	DKAK	19.017
AFDF	429.287	DALL	9.642	KDDF	18.877
DALD	427.785	AFLF	9.421	LAAK	18.781
DFAK	426.621	FFLA	9.370	ALLA	18.764
FLFD	426.511	DFLD	9.137	DFLA	18.708
FDKD	426.378	LADA	9.033	AFDA	18.401
DFDL	425.217	LDDD	8.727	LKFA	18.370
LFKL	423.984	FFFF	8.510	AFAK	18.314
AKLK	423.789	LLFK	8.410	AKDA	18.253
AFKF	423.476	DKKL	8.257	KADF	18.180
AFLA	423.462	AAAA	8.228	LDAK	17.777
DFKD	422.370	DDDF	8.092	KADL	17.452
DAFA	422.369	LFKF	8.085	DALD	17.307
ADLA	422.278	AFDF	8.040	LDFK	17.292
DLDK	421.769	AFLK	8.019	DLAL	17.085
ALAA	420.413	AAFL	7.970	LDKD	17.059
LFKF	419.896	FFDK	7.927	LALA	17.059
FKDK	419.179	LDFD	7.913	FFLF	17.024
LFAF	417.327	ALFF	7.861	DFKL	16.919
DAFD	416.107	AALA	7.755	LFDD	16.898
KDKL	416.093	LLKF	7.683	FFLL	16.892
DDKF	414.389	ADLK	7.682	DKFF	16.560
FALA	413.777	FFDD	7.658	FFAK	16.490

FAAK	412.450	DLLA	7.432	AADK	16.372
ALAL	408.706	LDKA	7.087	DKFK	16.352
ALFD	407.182	LDAF	6.724	LDKK	16.275
LLAK	405.241	LFDA	6.628	AKAA	15.911
DKDD	404.868	LKFL	6.533	LDLK	15.863
AALD	404.287	ADLL	6.422	DKDF	15.772
FFLK	403.870	AKFA	6.285	LDLA	15.755
ADFF	403.855	LFAA	6.130	LDAF	15.681
FLFK	403.348	KDDF	6.114	DAFL	15.571
LDKL	402.444	LAAD	6.114	FKLA	15.426
ADAD	401.840	KLAF	6.038	LLLA	15.421
AAKF	400.288	LKAD	6.020	LFKA	15.416
DFKA	399.473	DAFK	6.015	DDDA	15.252
DKDK	398.746	AFDL	5.705	AAAA	15.040
FDKF	398.563	AKFL	5.679	DFDL	14.787
DAAF	398.235	LFKD	5.472	DKLA	14.564
LFFL	397.890	DFFF	5.405	LKFK	14.481
DDDA	397.126	AFAA	5.386	DLFA	14.421
DADK	396.717	LDDF	5.217	ADFK	14.389
ADKL	394.903	DLAK	5.210	LFFK	14.200
DFDF	393.742	LKDD	4.842	DLDA	14.189
ALAK	390.355	AKDL	4.742	LDKF	14.109
LKAF	389.907	DLAL	4.600	FLDD	14.013
AFLD	389.854	DFKK	4.568	FFLD	14.004
KAFD	389.396	AFFL	4.508	DAFK	13.794
LAFK	388.430	LLKK	4.402	LLFA	13.642
FAKF	387.914	DDAF	4.161	LAFF	13.448
KDAA	387.472	FFLL	4.064	ADLD	13.433
AAFL	386.439	LKKK	4.059	LADL	13.062
FLDF	385.748	DLDK	4.053	FDL D	13.004
LDDA	385.158	DDAL	3.989	AFAA	12.828
LDDF	383.473	DLLD	3.939	AADA	12.455
AFDD	383.384	LAAA	3.921	ADFF	12.403
LFAD	382.067	AAFF	3.827	LDLD	12.184
AKAD	381.869	LDFA	3.826	DFFA	12.157
FKFD	380.074	LDAD	3.651	LALK	12.065
DDAA	379.737	DALF	3.647	ADLA	12.051
FDLK	378.717	FADK	3.600	DFKF	11.942
LFAK	377.968	FAKA	3.582	LAFK	11.937
FLKA	375.113	AAFK	3.505	LLDD	11.835
DFDK	374.564	DKLL	3.394	LDDL	11.828
FKDL	372.677	LAKF	3.216	AADF	11.535
FLAL	372.105	DLAA	3.187	FFAA	11.485
LDKF	371.288	ADLD	2.956	LFFL	11.374
FDKL	370.774	LLAA	2.604	DFKK	11.225
FDLA	369.472	DDDA	2.583	LKAA	11.218
FLDA	369.453	FKFA	2.485	DALF	10.986
LKDA	369.032	LKFF	2.354	AFFA	10.658
ADDA	368.610	DLFF	2.256	DLDK	10.444
AAKD	368.606	FFKD	2.177	DDAA	10.438

KDDL	367.569	DFKA	2.038	DDLK	10.417
AFAL	367.537	LDFL	1.856	DFDF	10.393
LADD	367.174	DAKK	1.780	AALK	10.361
DFAL	366.707	LADK	1.772	LKAK	10.205
LLLK	366.131	LFLD	1.728	DKLL	10.045
LKDK	366.054	DLLL	1.706	LDFA	9.998
LLDA	365.797	AFAL	1.621	LALD	9.880
DDAF	365.007	FDLF	1.611	AAFD	9.869
AKFD	363.709	LKAA	1.599	DKAL	9.846
AFFL	363.696	DAFL	1.557	ADAF	9.339
DFKK	361.549	ALLF	1.552	DFAF	9.279
AAAD	360.297	FALL	1.522	DFLF	9.228
KDAL	359.588	FDFL	1.393	FDKF	9.210
FKAA	356.587	FFDF	1.268	AKFD	9.175
DDFF	356.410	AKKA	1.212	DKLK	9.043
FDDD	356.373	AALK	1.099	AAAD	8.859
FLDK	355.956	LFAL	0.990	LKDL	8.786
FAAD	355.191	FFLD	0.572	LLDK	8.667
ALFK	353.889	AKLK	0.518	DFAA	8.666
AFAK	353.442	LKFA	0.435	LDLF	8.512
FOLD	352.875	FOLD	0.417	ADLF	8.458
DDFK	351.894	FAAF	0.409	FFDF	8.429
AFDL	351.181	AFLI	0.376	DLLA	8.067
FAKK	345.744	DALK	0.213	AFFD	7.940
FALK	344.504	AALL	0.145	AKLL	7.854
ADAK	344.432	AFAF	0.119	KDAL	7.623
FDAF	343.657	LKFK	0.119	KKDA	7.617
AAFD	343.480	LLLF	0.105	DLFL	7.523
DDDF	343.426	FALD	0.074	LDKA	7.302
ADDL	342.927	LLAD	0.000	LDAA	7.144
FADA	342.066	LLAF	0.000	AKAL	6.793
AKKK	341.081	LLAK	0.000	ADFD	6.648
FADL	338.604	LLAL	0.000	KALL	6.557
FLAK	338.346	LLDA	0.000	AKLD	6.510
LALD	338.289	LLDD	0.000	DALL	6.338
LAFD	337.666	LLDF	0.000	DAAA	6.309
ALDD	336.464	LLDK	0.000	FDLA	6.266
DFFK	332.061	LLDL	0.000	ADLL	6.087
AAAK	331.040	LLFA	0.000	FFLA	6.028
LKDD	330.685	LLFD	0.000	AFAD	5.750
LFKA	329.329	LLFF	0.000	LLFL	5.725
ALDK	328.977	LLFL	0.000	LFDF	5.641
FDKK	328.846	LLKA	0.000	DFLK	5.516
DDAL	328.449	LLKD	0.000	FDLL	5.499
DDDD	328.256	LLKL	0.000	LFAK	5.394
AKAA	327.204	LLLA	0.000	LFDL	5.364
DDKA	326.739	LLLK	0.000	AKLK	5.184
AALK	326.170	LLLL	0.000	AKFK	5.001
DDKD	325.565	LKAF	0.000	FFFA	4.839
AFAD	325.376	LKAK	0.000	FADK	4.788

AAKA	323.448	LKDA	0.000	LDDK	4.780
LFLD	322.843	LKDF	0.000	LLKL	4.704
LDLF	322.735	LKDK	0.000	FDLF	4.439
DDDL	319.866	LKDL	0.000	DDAF	4.382
DDFD	317.889	LKFD	0.000	DALK	4.339
ALDA	317.790	LKKF	0.000	LDDF	4.320
AKDD	317.276	LKLA	0.000	LDDD	4.055
LFFA	317.064	LKLL	0.000	FFAL	4.000
FAKA	316.991	LFAD	0.000	AADL	3.993
AFAF	316.849	LF AF	0.000	LLDF	3.948
LLDK	316.365	LFAK	0.000	FALF	3.799
AKKD	315.681	LFDD	0.000	LKAD	3.783
AKAL	314.307	LFDK	0.000	AALD	3.674
AFDA	311.704	LFFA	0.000	DLLD	3.620
FKAL	309.680	LFFD	0.000	A AFF	3.448
AAKK	308.819	LFFK	0.000	LKFD	3.375
FLFA	308.546	LFKK	0.000	LLLK	3.109
DLDF	306.531	LFKL	0.000	DDFD	2.911
FFAA	306.489	LFLA	0.000	AFDL	2.744
DAAL	306.470	LFLK	0.000	FFKA	2.677
LDLA	306.056	LFLL	0.000	FAKA	2.532
AFKD	305.899	LDAK	0.000	DFFK	2.531
LKKK	304.787	LDDA	0.000	ADLK	2.519
AFKK	303.319	LDDK	0.000	AFFL	2.446
LLAL	302.012	LDDL	0.000	FAKF	2.408
ALDF	299.574	Ldff	0.000	LKKA	2.312
AFFD	297.619	LDFK	0.000	FALA	2.130
FALD	296.824	LDKL	0.000	ADDL	2.015
ADDK	296.014	LDLA	0.000	DLKF	1.956
FKFK	295.855	LDLD	0.000	LFFD	1.945
AAFK	293.705	LDLK	0.000	FAAA	1.861
AKFK	290.250	LDLL	0.000	LFAD	1.535
FFAD	288.317	LAAF	0.000	LFFA	1.292
DAAA	286.304	LA AK	0.000	DLFF	1.139
AFLK	285.573	LAAL	0.000	LALL	1.073
DAFK	284.948	LADF	0.000	DLFK	1.039
DAFF	282.482	LAFF	0.000	LLLD	1.003
ADLD	281.831	LALF	0.000	AFFF	0.973
FDDA	281.723	KKDA	0.000	ADDA	0.966
ADKF	281.708	KFAK	0.000	DDKK	0.916
AAAL	280.360	FLLA	0.000	FAFL	0.827
LDDD	280.100	FKLA	0.000	LKKL	0.683
AAAF	280.099	FFDA	0.000	FAFA	0.548
DDDK	279.526	FFKA	0.000	LDFL	0.471
LFKD	278.351	FFLK	0.000	LADK	0.352
FLAA	276.888	FDAF	0.000	LKLF	0.315
AKDA	274.994	FDDF	0.000	DFLD	0.211
FDDK	274.608	FDFA	0.000	AKFF	0.194
AKAK	274.225	FDFF	0.000	LLAA	0.000
LFFD	274.068	FDFK	0.000	LLDA	0.000

LFFK	273.653	FDKA	0.000	LLKD	0.000
LAFF	271.056	FDKD	0.000	LLKF	0.000
FDAK	270.281	FDKF	0.000	LLLL	0.000
FFFF	269.422	FDKK	0.000	LKAL	0.000
FFDD	268.846	FDKL	0.000	LKDF	0.000
ADKD	266.964	FDLA	0.000	LKFL	0.000
DDKK	265.540	FDLK	0.000	LKKF	0.000
AFKA	263.205	FDLL	0.000	LKLL	0.000
AKDK	261.490	FADF	0.000	LFAA	0.000
ADAF	260.841	FAFA	0.000	LFAF	0.000
FFFD	260.111	FAFF	0.000	LFAL	0.000
FFKL	258.549	FAFK	0.000	LFDK	0.000
LDKA	257.861	FAFL	0.000	LFKD	0.000
ADFL	256.890	FAKD	0.000	LFKF	0.000
FAAL	255.202	FAKF	0.000	LFLK	0.000
AKKA	254.612	FAKK	0.000	LFLK	0.000
AFAA	254.571	FAKL	0.000	LDAD	0.000
LFLK	253.906	FALA	0.000	LDAL	0.000
FADD	251.798	FALF	0.000	LDLL	0.000
FFDF	239.924	DLDF	0.000	LAAA	0.000
FDKA	239.331	DLFK	0.000	LAFF	0.000
ADKA	236.850	DLFL	0.000	LAAL	0.000
AFFA	235.253	DLKA	0.000	Lafa	0.000
ADFA	234.225	DLKD	0.000	LAKF	0.000
ADFD	233.841	DLKF	0.000	LAKK	0.000
FFKD	233.055	DLKK	0.000	LALF	0.000
AFFK	232.880	DLKL	0.000	FFDA	0.000
ADDF	232.088	DLLF	0.000	FFLK	0.000
AFDK	231.092	DKFF	0.000	DFDK	0.000
FFKK	229.822	DKFK	0.000	FDKA	0.000
LDLD	221.448	DKLA	0.000	FDKD	0.000
FDFD	221.241	DFAL	0.000	FDKK	0.000
LAFF	219.851	DFDF	0.000	FADF	0.000
FADF	219.379	DFFK	0.000	FAFF	0.000
FDFD	219.213	DFFL	0.000	FAFK	0.000
FADK	218.590	DFKL	0.000	FAKD	0.000
FDDL	218.357	DFLA	0.000	FAKK	0.000
FFDA	218.195	DFLF	0.000	FAKL	0.000
FAAF	217.660	DFLL	0.000	FALL	0.000
FFFL	216.329	DDAA	0.000	DLDF	0.000
FAFD	216.181	DDFK	0.000	DLKA	0.000
KAAA	215.810	DDFL	0.000	DLKD	0.000
DFDK	215.741	DDKA	0.000	DLKK	0.000
FFAF	207.680	DDKD	0.000	DLKL	0.000
LDKD	206.220	DDKF	0.000	DLLF	0.000
FFFK	202.108	DDKK	0.000	DLLK	0.000
FAFA	200.824	DDKL	0.000	DLLL	0.000
FDFA	200.409	DDLA	0.000	DFAK	0.000
ADDD	198.903	DDLD	0.000	DFDK	0.000
ADLK	198.220	DDLf	0.000	DFFL	0.000

LKAA	197.712	DDLK	0.000	DFKA	0.000
FAFL	195.444	DDLL	0.000	DFLL	0.000
ADFK	193.712	DAAA	0.000	DDAK	0.000
ADKK	193.334	DALA	0.000	DDAL	0.000
FDDF	192.608	ALLA	0.000	DDDF	0.000
FFDK	192.262	AKAA	0.000	DDDL	0.000
LDKK	192.196	AKFF	0.000	DDFL	0.000
FFKF	190.699	AKFK	0.000	DDKA	0.000
FDFL	185.675	AKLA	0.000	DDKF	0.000
FDAL	180.089	AKLD	0.000	DDKL	0.000
LDAF	179.112	AFDA	0.000	DDLDF	0.000
LDLK	176.141	AFFA	0.000	DDLL	0.000
FFAL	174.457	AFFF	0.000	DAAL	0.000
FFDL	174.417	AFFK	0.000	AKFA	0.000
AAAA	172.908	AFLA	0.000	AFAF	0.000
FFFA	172.279	ADAA	0.000	AFAL	0.000
ADAA	170.375	ADAL	0.000	AFDF	0.000
LFKK	161.858	ADDA	0.000	AFFK	0.000
FAFK	160.881	ADDF	0.000	AFLA	0.000
ALAF	159.031	ADFA	0.000	AFLF	0.000
FAAA	156.906	ADFD	0.000	AFLL	0.000
LAKK	156.465	ADFF	0.000	ADAA	0.000
LAAL	131.279	ADFK	0.000	ADAL	0.000
FFKA	128.215	ADLA	0.000	ADDF	0.000
FAFF	121.035	AAAL	0.000	ADFA	0.000
LAAA	111.767	AADA	0.000	AAAL	0.000
KKDA	89.877	AADF	0.000	AAFA	0.000
ADAL	67.838	AADK	0.000	AAFK	0.000
FDAF	0.000	AADL	0.000	AAFL	0.000
ALLA	0.000	AAFA	0.000	AALF	0.000
AKLA	0.000	AAFD	0.000	AALL	0.000